AAPPS Bulletin

ORIGINAL ARTICLE Open Access

Time-resolved secondary triton burnup 14 MeV neutron measurement by a new scintillating fiber detector in middle total neutron emission ranges in deuterium large helical device plasma experiments

K. Ogawa[1,2*], M. Isobe[1,2], S. Sangaroon[1,3], E. Takada[4], T. Nakada[4], S. Murakami[5], J. Jo[6], G. Q. Zhong[7], Yipo Zhang[8], S. Tamaki[9] and I. Murata[9]

Abstract

A middle-sensitivity scintillating fiber detector (hereafter middle Sci-Fi detector) that works at a deuterium-tritium neutron flux of ~10^5-10^7 $cm^{-2}s^{-1}$ was utilized to measure secondary deuterium-tritium neutron emission rates with high temporal resolution at a total neutron emission rate of 10^{13} to 10^{15} n/s, where strong magnetohydrodynamic (MHD) instabilities were observed in the large helical device deuterium plasma experiments. The gain and angular characteristics of the middle Sci-Fi detector were evaluated in an accelerator-based deuterium-tritium neutron source in the intense 14 MeV neutron source facility at Osaka University. Observation of 1 MeV triton transport due to MHD instability was performed by a middle Sci-Fi detector whose deuterium-tritium neutron counting rate was approximately 20 times higher than that of the conventional Sci-Fi detector. Fusion-born triton transport due to energetic-particle-driven MHD instability was observed using the middle Sci-Fi detector due to its high detection efficiency and high discrimination ability of deuterium-tritium neutrons from the sea of deuterium-deuterium neutrons.

Keywords: Neutron measurement, Scintillating fiber, Triton burnup, Fusion plasma

1 Introduction

Energetic particle confinement is one of the issues for achieving and sustaining a deuterium-tritium (DT) fusion burning plasma because the plasma is mainly heated by alpha particles created by DT fusion reactions. Research on energetic particle confinement in magnetic confinement fusion devices has been intensively performed to realize a fusion reactor [1, 2]. In plasma experiments using deuterium gas, the behavior of a 1 MeV triton created by the deuterium-deuterium reaction has been intensively studied because the 1 MeV triton can be regarded as an alpha particle. The initial velocity distribution of 1 MeV triton is almost as isotropic as the distribution of alpha particles. Additionally, the Larmor radius and precession frequency of the trapped 1 MeV triton are almost the same as those of 3.5 MeV alpha particles. The triton burnup ratio, that is, the secondary DT neutron emission yield divided by the DD neutron emission yield, which is almost the same as the 1 MeV triton yield, is used as the index of the triton confinement ability of fusion devices. A relatively high DT neutron emission rate indicates that tritons slow properly because the DT reaction cross section has a peak of

* Correspondence: ogawa.kunihiro@nifs.ac.jp
[1]National Institute for Fusion Science, National Institutes of Natural Sciences, Toki, Japan
[2]The Graduate University for Advanced Studies, SOKENDAI, Toki, Japan
Full list of author information is available at the end of the article

approximately 100 keV. Shot-integrated triton burnup ratio research has been performed mainly by neutron activation systems to show alpha confinement capability in existing magnetic confinement fusion devices [3–11]. The other important topic is the transport of alpha particles due to the magnetohydrodynamic (MHD) instabilities in a fusion reactor. Measuring the time evolution of the DT neutron emission rate in existing devices is required to contribute to understanding MHD instability-induced alpha particle transport in a fusion reactor. Even though the neutron activation system provides the absolute value of the triton burnup ratio because neutron activation is insensitive to gamma-rays, time-resolved measurement with ms order is impossible. Therefore, to perform time-resolved measurements of the DT neutron emission rate, scintillating fiber (Sci-Fi) detectors were developed for the Tokamak Fusion Test Reactor (TFTR) and Japan Torus-60 (JT-60U) in the 1990s [12, 13]. Here, the Sci-Fi detector works based on pulse-height discrimination, and the operational range with reasonable time resolution ms order becomes possible over a range of almost two orders of magnitude. The original Sci-Fi detectors were utilized for high total neutron emission rate (S_n) conditions exceeding 10^{16} n/s.

In the deuterium experiment performed in the large helical device (LHD) [14–16], energetic particle confinement studies are largely advanced using a variety of neutron diagnostics [17–23]. Sci-Fi detectors play a part in comprehensive neutron diagnostics. To measure the time-resolved spatial profile of triton confinement, compact Sci-Fi detectors, which are suitable for preparing detector arrays and have a sensitivity similar to that of the original Sci-Fi detector for DT neutron profile measurement [24–28], have been developed. The compact Sci-Fi detectors operate at S_n values of ~10^{15} n/s to ~10^{17} n/s. In the LHD, plasma discharge with MHD instabilities possessing relatively large amplitudes is excited in the S_n range of 10^{13} n/s to 10^{15} n/s [29, 30]. Although beam ion transport due to MHD instabilities has been intensively studied by vertical neutron cameras [18–20], the effect of deuterium-deuterium (DD) fusion-born triton transport is unclear because there is almost no DT neutron count in vertical neutron cameras [31]. To understand the DD fusion-born triton transport due to the MHD instabilities, time-resolved measurement of secondary DT neutrons with a 1 ms time bin over this S_n range is required. For DT neutron measurement in discharges with MHD instabilities, a high-detection-efficiency Sci-Fi detector for low S_n discharge [32] was developed. Although the number of Sci-Fi detectors must be ~500 times larger than that of the compact Sci-Fi detector to enhance the detection efficiency by ~500 times, experiments showed that the operational range of S_n of the sizable detector is approximately 10^5 times lower than that of the compact Sci-Fi detector, i.e., an S_n value of ~10^{10} to ~10^{12} n/s in the LHD due to the relatively low directivity of ~50 degrees. This manuscript shows the characterization of a new middle-sensitivity Sci-Fi detector (hereafter middle Sci-Fi detector) for understanding DD fusion born-triton transport due to MHD instabilities, where S_n values of ~10^{13} n/s to ~10^{15} n/s in the LHD correspond to a DT neutron flux 10^5-10^7 $cm^{-2}s^{-1}$ at the torus hall. This detector can be utilized at S_n values of ~10^{13} n/s to ~10^{15} n/s, i.e., Wendelstein 7-X [33], EAST [34], and HL-2M [35].

2 A middle scintillating fiber detector

First, the concept of the Sci-Fi detector is explained briefly. In deuterium plasma discharges in magnetic confinement fusion experiments, the typical triton burnup ratio is 1%. Therefore, the DD neutron flux is almost two orders of magnitude higher than the DT neutron flux. To discriminate the DT neutron-induced signal from the significant DD neutron-induced signal, the pulse height discrimination method is utilized. Additionally, in the fast-neutron detector, stray neutrons and gamma-rays can result in unwanted pulse counts. The directivity of the detector is implemented to reduce the stray radiation effect because DT neutrons come from the front side where the plasma core region exists. Sci-Fi is used to implement the directionality of the detector. Although the directionality is not so intense, the directionality effectively reduces the unwanted counts. In addition, between the Sci-Fi detectors, a recoiled particle and gamma-ray absorber prepared from an aluminum substrate is implemented. Therefore, a pulse with a high height can only be achieved when the DT neutron comes from the front side and the recoiled proton goes

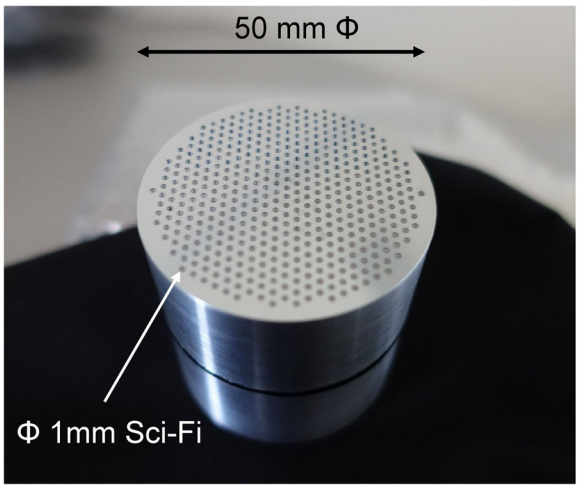

Fig. 1 The head of the middle Sci-Fi detector. A total of 456 scintillation fibers with a length of 5 cm were embedded into the aluminum substrate

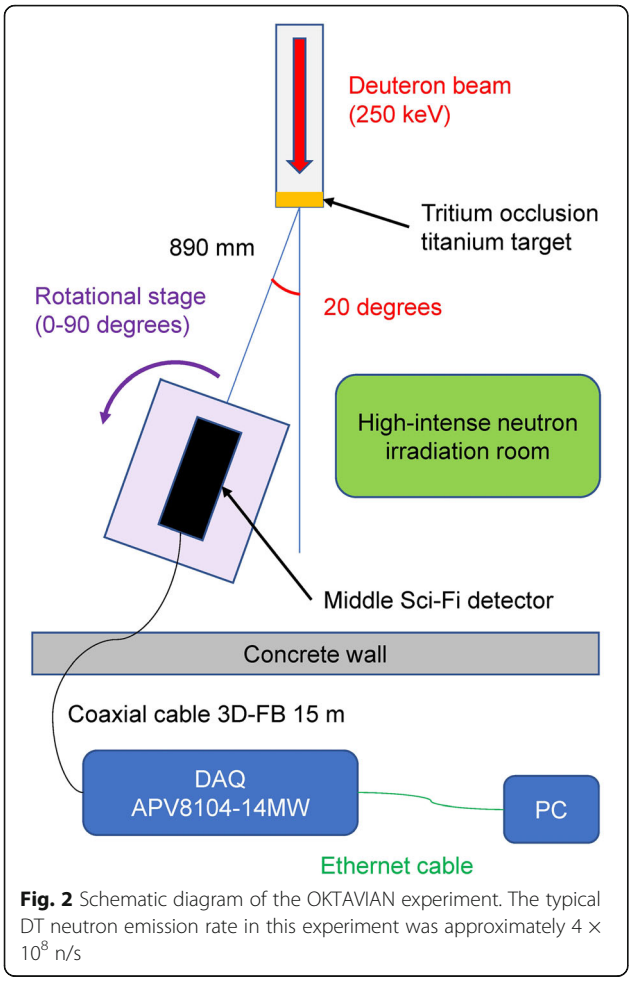

Fig. 2 Schematic diagram of the OKTAVIAN experiment. The typical DT neutron emission rate in this experiment was approximately 4 × 10^8 n/s

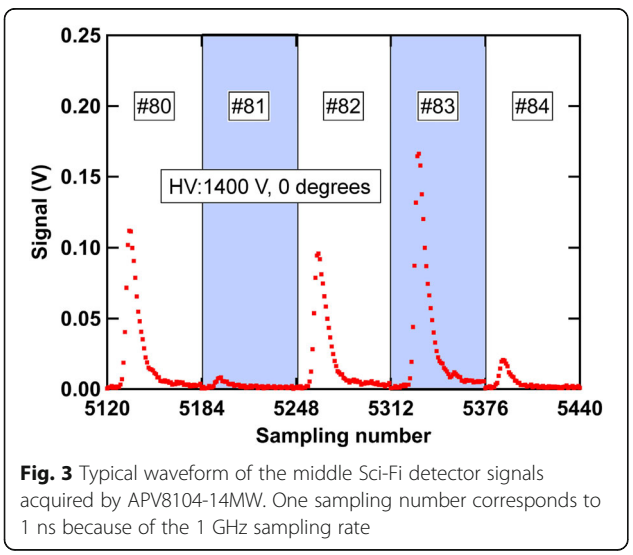

Fig. 3 Typical waveform of the middle Sci-Fi detector signals acquired by APV8104-14MW. One sampling number corresponds to 1 ns because of the 1 GHz sampling rate

along the Sci-Fi detector. On the other hand, low-energy neutrons or gamma-rays result in a small pulse.

Figure 1 shows the external view of the head part of a middle Sci-Fi detector. A total of 456 BCF-10 (Saint-Gobain K. K.) Sci-Fis with a 1-mm diameter are embedded into the aluminum substrate. The Sci-Fi length of 5 cm is chosen based on a previous study [36]. The detection efficiency of the Sci-Fis toward fast neutrons becomes almost saturated at this length due to the so-called self-shielding effect. The reason for embedding a relatively large number of Sci-Fis is to enhance the detection efficiency. The reason for choosing 456 Sci-Fis is

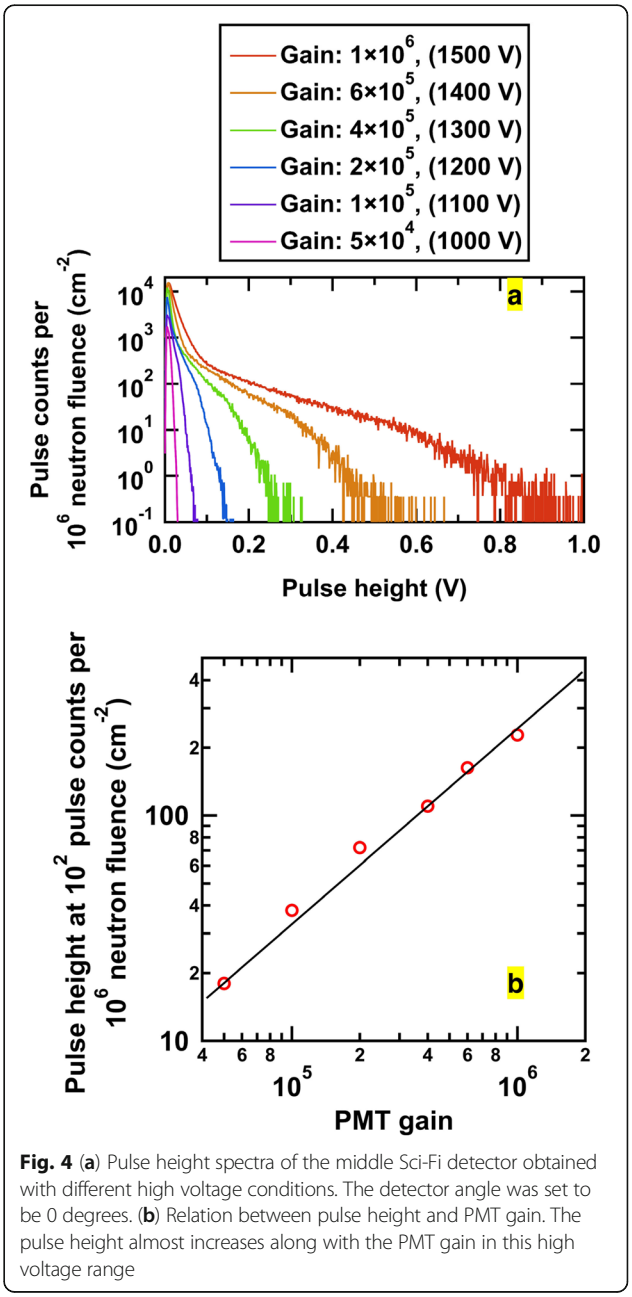

Fig. 4 (**a**) Pulse height spectra of the middle Sci-Fi detector obtained with different high voltage conditions. The detector angle was set to be 0 degrees. (**b**) Relation between pulse height and PMT gain. The pulse height almost increases along with the PMT gain in this high voltage range

to aim for the detection efficiency between that of a compact Sci-Fi detector with ~100 Sci-Fis and a sizable Sci-Fi detector with ~5000 Sci-Fis. The Sci-Fi head is coupled with a conventional 2-inch photomultiplier tube (PMT, H7195, Hamamatsu K. K.). The anode signal of the PMT is directly fed into a 1 GHz sampling rate data acquisition system (DAQ) (APV8102-14MWPSAGb or its old version APV8104-14 MW, Techno AP Corp.), which is the same DAQ used as vertical neutron camera 1 in the LHD [31]. The pulse height analysis involves postprocessing using 64 data points.

3 Test of the middle Sci-Fi detector in an accelerator-based deuterium-tritium neutron generator

Characterization of the middle Sci-Fi detector was performed in a high-intensity neutron irradiation room in an intense 14 MeV neutron source facility (OKTAVIAN) at Osaka University [37]. Figure 2 shows a schematic drawing of the experiment. Deuteron beams with ~250 keV were injected into the tritium occlusion titanium target. The neutron energy at the middle Sci-Fi detector position was evaluated to be 15.2 MeV. The middle Sci-Fi detector was loaded on the rotational stage. The 0 degree means that the Sci-Fi detector is directed to the neutron source, and 90 degrees means that the Sci-Fi detector axis follows the tangential line. The middle Sci-Fi detector signal was transferred to a DAQ placed outside of the high-intensity neutron irradiation room using a 15 m 3D-FB 50 Ohm cable, which is the same cable impedance and length used in the LHD experiment.

The gain characteristics of the middle Sci-Fi detector were obtained at the rotational stage angle of 0 degrees to check whether the linearity of the pulse was fulfilled under these operational conditions. The pulse height discrimination is not valid if gain variation occurs. Figure 3 shows the typical waveform of pulse signals obtained at a high voltage of 1400 V. The rise and fall times of the scintillation pulse are ~5 ns and ~7 ns, respectively. In the pulse height postanalysis, the maximum height at 64 points was searched. Figure 4 a shows the result of the high voltage scan. In this figure, the typical gain together with the high voltage shown in the catalog is indicated. The pulse height becomes more significant with increasing high voltage, as expected. The knee in the pulse height is observed at a high voltage of 1100 V to 1500 V. Such a pulse height spectral shape is characteristic of a Sci-Fi detector. To check the gain of the PMT, the pulse height at pulse counts per 10^6 neutron fluence equal to 100 is plotted as a function of the PMT gain, as shown in Fig. 4 b. The

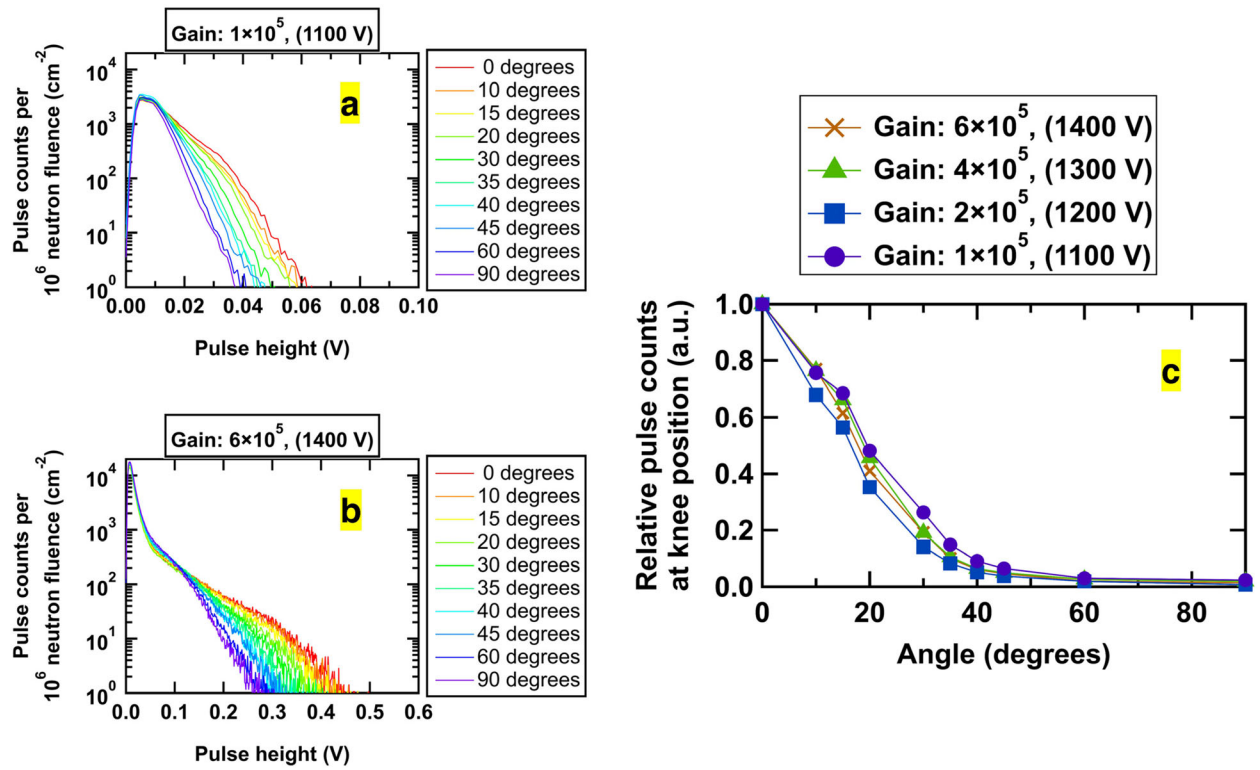

Fig. 5 Pulse height spectra of the middle Sci-Fi detector obtained with changing detector angles at (**a**) a high voltage of 1100 V and (**b**) a high voltage of 1400 V. (**c**) Angular response of the middle Sci-Fi detector. The full-width at half-maximum of angle is 30-40 degrees

linearity of the PMT for a single pulse is maintained at a high voltage from 1000 to 1500 V.

The angular response of the middle Sci-Fi detector was obtained by varying the detector angle using the rotational stage. At the high voltage of 1100 V shown in Fig. 5 a, a knee appeared at the pulse height of ~0.03 V. The pulse counts of the knee are one order smaller than those of low-height components, which are due to gamma-rays and scattering neutrons. Figure 5 b shows the dependence of relative pulse counts as a function of the detector angle. Here, pulse counts at the knee position were chosen. The pulse counts are normalized by the pulse counts at the detector angle of 0 degrees. The directionality is almost unchanged regardless of the high voltage setting because the directionality is decided by the detector geometry. The full-width half-maximum of the relative pulse counts shows that the directionality of

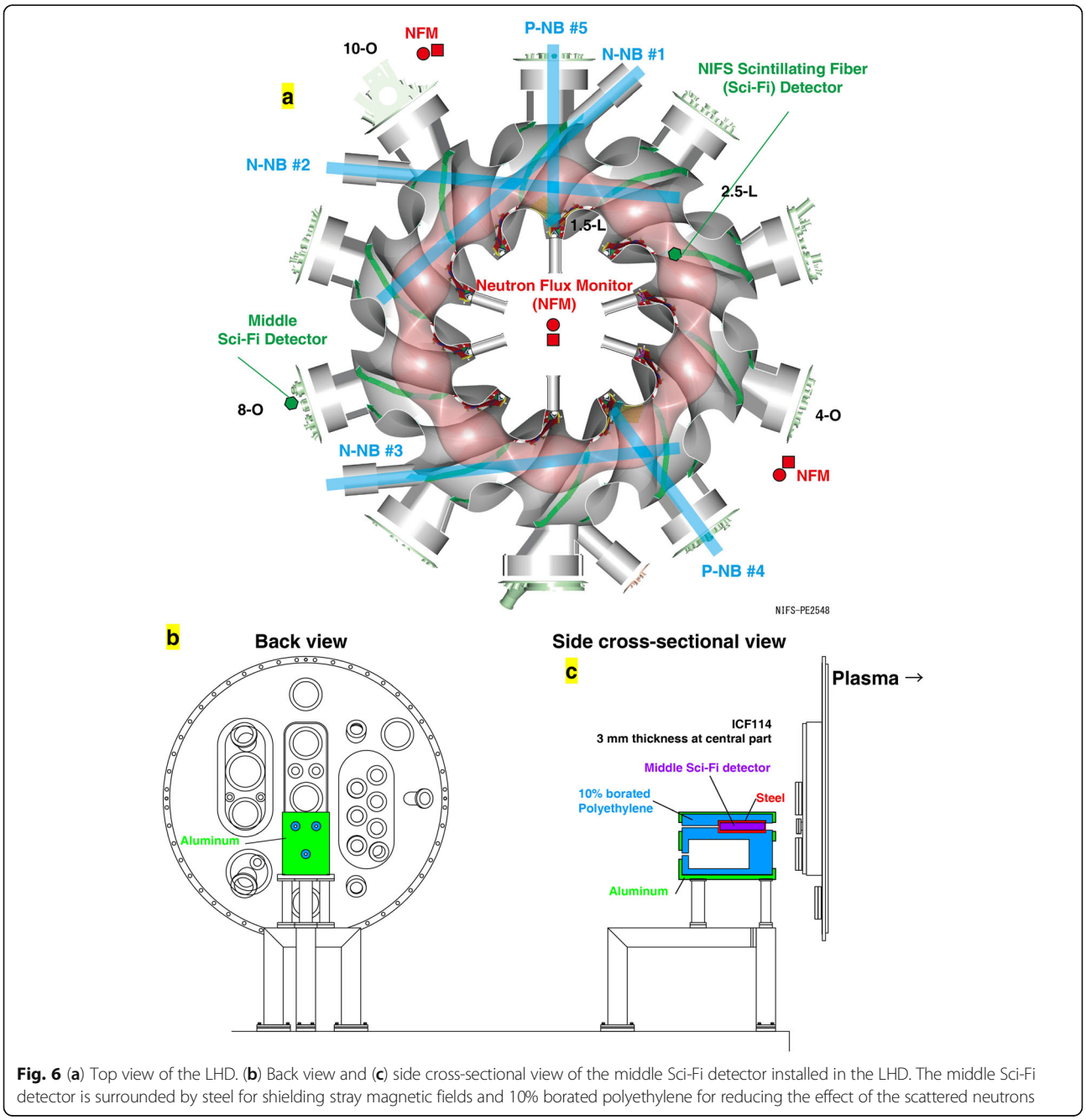

Fig. 6 (**a**) Top view of the LHD. (**b**) Back view and (**c**) side cross-sectional view of the middle Sci-Fi detector installed in the LHD. The middle Sci-Fi detector is surrounded by steel for shielding stray magnetic fields and 10% borated polyethylene for reducing the effect of the scattered neutrons

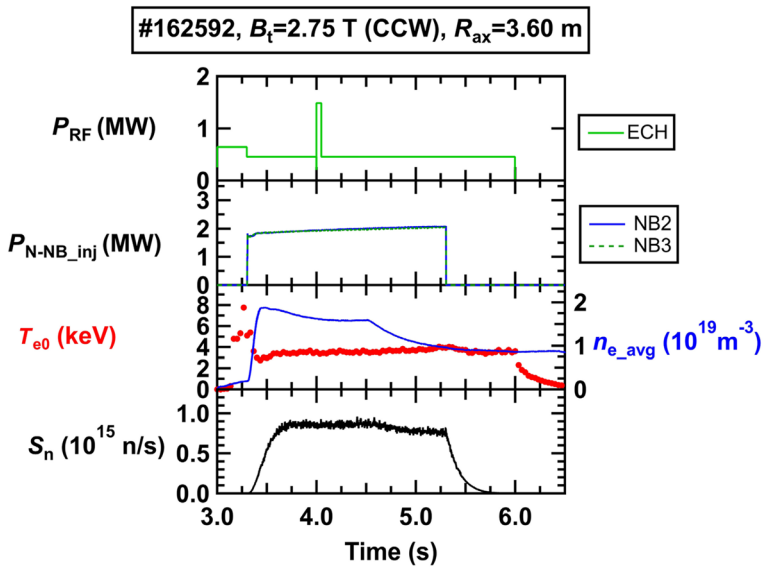

Fig. 7 Time evolution of triton burnup discharge. Deuterium NBs were injected into plasma sustained by ECH. The injection powers of NB2 and NB3 were almost the same

the middle Sci-Fi detector is 30-40 degrees, which is better than that of the sizeable Sci-Fi detector [32].

4 Secondary deuterium-tritium neutron measurement in the LHD

4.1 Arrangement of a scintillating fiber detector in the LHD

Secondary DT neutron measurement at an S_n value of ~10^{15} n/s using a middle Sci-Fi detector was performed in the LHD. Figure 6 a shows the bird's-eye view of the LHD. Three negative-ion-based neutral beam injectors (N-NB #1 to #3) and two positive-ion-based neutral beam injectors (P-NB#4 and P-NB #5) were used in this experiment. The neutron flux monitor was utilized to measure S_n [38, 39]. The National Institute for Fusion Science (NIFS) Sci-Fi detector installed on the bottom of the LHD (2.5-L port) was used to compare DT neutron measurements [24]. The middle Sci-Fi detector is installed on the outboard side of the LHD (8-O port). The expected neutron flux is approximately four times higher in the 8-O port than in the 2.5 L port due to the distance from the plasma to the detector [40]. Figures 6 b and c show the back view and the side cross-sectional view of the middle Sci-Fi detector in the LHD. It is worth noting that the ICF114 port in front of the middle Sci-Fi detector has a 3-mm thickness at the central part to reduce the neutron scattering effect. The middle Sci-Fi detector is covered by steel (SS400) to shield the PMT from the stray magnetic field. To reduce the scattering neutrons coming from the side and the back of the detector, a neutron shield composed of 10% borated polyethylene is additionally adopted.

4.2 Comparison with existing neutron detectors

The experiment was performed at a high magnetic field and the inward shifted configuration, where relatively high triton confinement performance is expected [41]. The magnetic field strength at the magnetic axis position (B_t) is set to 2.75 T with the counterclockwise direction from the top view, and the preset of the magnetic axis position (R_{ax}) is set to 3.60 m. Electron cyclotron heating (ECH) initiates a deuterium plasma with 0.6 MW. After plasma initiation, N-NBs #2 and #3 are injected (Fig. 7). The central electron temperature (T_{e0}) is 3 to 4 keV, except for the early and end phases of discharge. The line-averaged electron density (n_{e_avg}) shows that n_{e_avg} is approximately 2 × 10^{19} m^{-3} in the N-NB injection phase. From t of 3.5 s, n_{e_avg} gradually decreases and reaches 1 × 10^{19} m^{-3} at t of 5.0 s. The time evolution of S_n shows that S_n gradually increases up to 9 × 10^{14} n/s with N-NB#3 injection and becomes almost constant from t of 3.75 s to 4.5 s. Then, S_n exponentially decays from t of 5.3 s due to the cessation of N-NB injections. Figure 8 a shows the pulse height spectra of the middle Sci-Fi detector signal obtained in #162592 at t of 3.3 to 6.0 s. The pulse height spectra have two components. The lower height component is mainly due to gamma-rays and low-energy neutrons, whereas the higher height component is mainly due to DT neutrons. From the pulse height spectra, the discrimination level suitable for the LHD experiment is found to be 70 mV at a high voltage

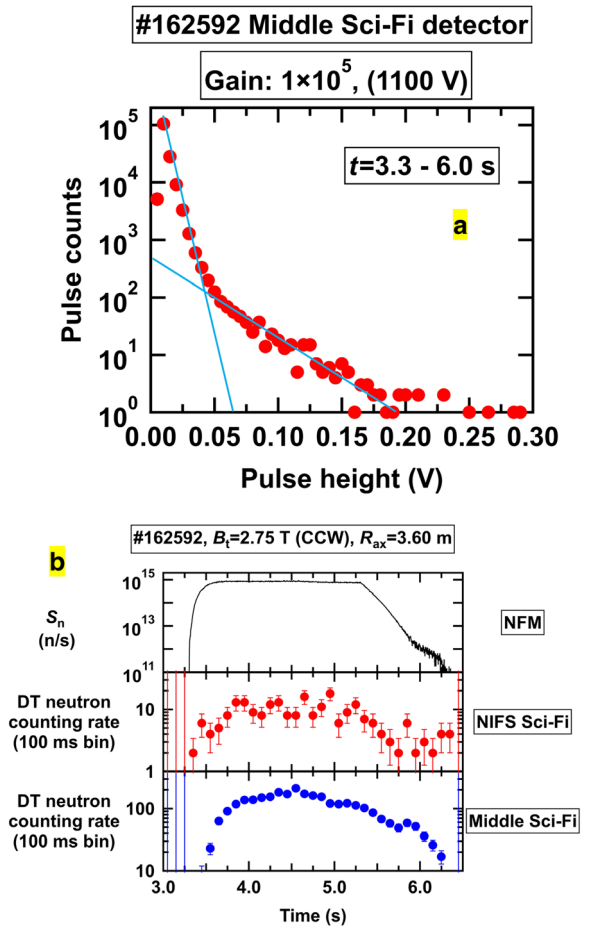

Fig. 8 (**a**) Pulse height spectra of the middle Sci-Fi detector obtained in the LHD experiment. The lower height component is mainly due to gamma-rays and low-energy neutrons, whereas higher height components are mainly due to DT neutrons. (**b**) Comparison of time evolutions of the total neutron emission rate (S_n), DT neutron counting rate obtained by the NIFS Sci-Fi detector, and DT neutron counting rate obtained by the middle Sci-Fi detector. The DT neutron counting rate is almost 20 times higher than that in the middle Sci-Fi detector compared with the conventional NIFS Sci-Fi detector

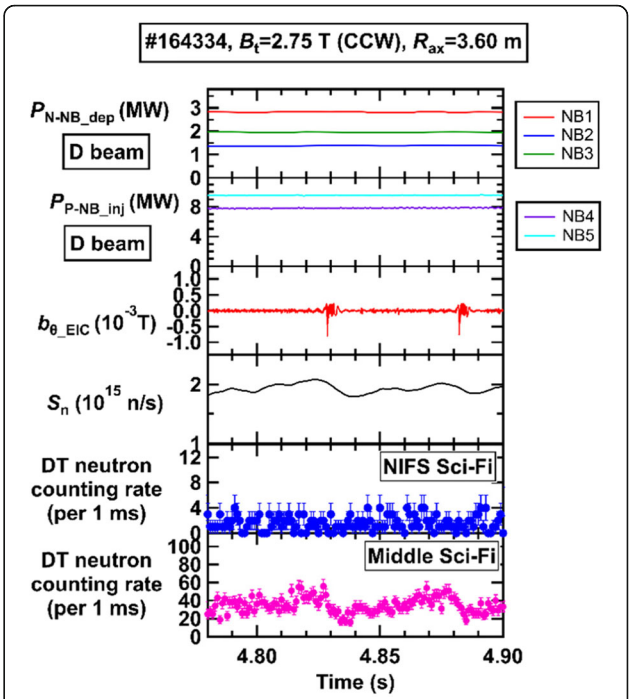

Fig. 9 Time evolution of LHD deuterium discharge with MHD instability. The drop in DT neutron flux is successfully obtained by the middle Sci-Fi detector

of 1100 V. A high voltage of 1100 V was chosen to measure S_{n_DT} at S_n of 10^{15} n/s, where the typical pulse counting rate is 7×10^4 cps. Note that the pulse height is large compared with the pulse height obtained in OKTAVIAN. A possible reason is the gain of the PMT because the PMTs used in OKTAVIAN and LHD are not identical. The gain of the PMT used at the LHD is almost two times higher than that used in OKTAVIAN. Figure 8 b shows the time evolution of S_n as well as the DT neutron counting rate per 100 ms bin for the NIFS Sci-Fi and middle Sci-Fi detectors. Here, the discrimination level for the NIFS Sci-Fi detector and the middle Sci-Fi detector was set to 300 mV and 70 mV, respectively. The rise and decay of the DT neutron counting rate obtained by the Sci-Fi detectors are slower than S_n. The time evolution of S_n is dominated by the DD neutron emission rate because the energy response of the neutron flux monitor is almost flat over this neutron energy range, whereas the Sci-Fi detector signal is composed of the DT neutron emission rate. The difference in time traces can be explained by the DD and DT fusion cross sections. The total neutron emission rate is dominated by the reaction between beam deuterons and thermal deuterons. The fusion cross section monotonically rises within this energy range. In contrast, the DT neutron counting rate is dominated by the reaction between DD fusion-born tritons having 1 MeV of energy and thermal deuterons. Therefore, the deuterium-tritium fusion rate increases during the slowing down from 1 MeV. The typical counting rate of the NIFS Sci-Fi detector is ~10 counts for 100 ms. The error bar caused by the statistics of the count is ~30%. In addition, the typical counting rate of the middle Sci-Fi detector is ~200 counts for 100 ms. The error bar caused by the statistics of the count is ~7%. The pulse counts obtained with the middle Sci-Fi detector are approximately 20 times higher than those obtained with the NIFS Sci-Fi detector.

4.3 Observation of 1 MeV triton transport due to magnetohydrodynamic instabilities

We applied the middle Sci-Fi detector in the plasma discharge with MHD instabilities. Here, the experiment is

performed in relatively low-density plasma, where n_{e_avg}~1.0 × 10^{19} m^{-3}. Figure 9 shows the discharge waveform. In this discharge, all the NBs are injected into the plasma. The amplitude of magnetic fluctuation measured by the magnetic probe located on the vacuum vessel shows that bursting MHD instabilities are observed at t values of ~4.83 s and 4.88 s. The time evolution of S_n shows that S_n rapidly decreases due to MHD instabilities. The main components of the decrease in S_n are due to the transport of beam ions. The effect of MHD instabilities on DT neutron flux measured by the NIFS Sci-Fi detector is invisible because the typical DT neutron counting rate per 1 ms is approximately two. In addition, the drop in DT neutron flux due to the MHD instabilities is visible in the measurement by the middle Sci-Fi detector. The time evolution shows that the decay time of DT neutron flux due to the MHD instabilities is approximately 7 ms, which is shorter than that of DD neutron flux measured in S_n ~ 10 ms. The result suggests that fusion-born triton transport due to the MHD instability is relatively rapid compared with beam ion transport. Detailed analysis of DD fusion-born triton transport due to MHD instability is future work.

5 Summary

To understand MHD instability-induced fusion-born transport, a middle Sci-Fi detector that covers a DT neutron flux of 10^5 to 10^7, which corresponds to an S_n value of 10^{13} to 10^{15} n/s in the LHD, was developed. The characteristics of the middle Sci-Fi detector were surveyed in the accelerator-based DT neutron source OKTAVIAN. The linearity of the middle Sci-Fi detector is maintained over this operational high-voltage range of the PMT. Time-resolved measurement of DT neutron flux was performed in the LHD. The counting rate of the DT neutron signal obtained by the middle Sci-Fi detector was compared to the conventional NIFS Sci-Fi detector and S_n. The DT neutron counting rate becomes 20 times higher than that of the NIFS Sci-Fi detector. DT neutron emission rate measurement with high temporal resolution becomes newly possible by employing a middle Sci-Fi detector. The discrimination of 14 MeV neutrons from many 2.5 MeV neutrons and gamma-rays through pulse height discrimination with Sci-Fis enables a new observation of fusion product transport.

Acknowledgements

We are pleased to acknowledge the assistance of the LHD Experiment Group.

Authors' contributions

K. O. and M. I. conceived of the presented idea. M. I and S. M. supervised the project. K. O., M. I., E. T., and T. N. performed the study design. J. J., G. Q. Z, and Y. Z. were involved in planning the work. K. O., S. S., S. T., and I. M. carried out the experiments. K. O. wrote the draft of the manuscript. All authors discussed the results and contributed to the final manuscript. The author(s) read and approved the final manuscript.

Funding

This research was supported by the NINS program of Promoting Research by Networking among Institutions (Grant Number 01411702), NIFS Collaboration Research programs (KOAH033), Japan-Korea Fusion Collaboration Program, the Japan-China Post-Core-University-Program and Post-CUP.

Availability of data and materials

All data generated or analyzed during this study are included in this published article.

Declarations

Ethics approval and consent to participate

Not applicable

Consent for publication

Not applicable

Competing interests

The authors declare that they have no known competing financial interests or personal relationships that could have appeared to influence the work reported in this paper.

Author details

[1]National Institute for Fusion Science, National Institutes of Natural Sciences, Toki, Japan. [2]The Graduate University for Advanced Studies, SOKENDAI, Toki, Japan. [3]Mahasarakham University, Maha Sarakham, Thailand. [4]National Institute of Technology, Toyama College, Toyama, Japan. [5]Kyoto University, Kyoto, Japan. [6]Korea Institute of Fusion Energy, Daejeon, Republic of Korea. [7]Institute of Plasma Physics Chinese Academy of Sciences, Hefei, China. [8]Southwestern Institute of Physics, Chengdu, China. [9]Osaka University, Suita, Japan.

Received: 25 April 2021 Accepted: 26 July 2021
Published online: 24 August 2021

References

1. Fasoli A. et al 2007 Nuclear Fusion **47** S264. https://doi.org/10.1088/0029-5515/47/6/S05
2. Heidbrink W. W. and Sadlers G. J., 1994 Nucl. Fusion **34** 535. **23** 917. https://doi.org/10.1088/0029-5515/34/4/I07
3. Barnes C. W. et al 1998 Nucl. Fusion **38** 597. https://doi.org/10.1088/0029-5515/38/4/310
4. Conroy S. et al 1988 Nucl. Fusion **28** 2127. **23** 917. https://doi.org/10.1088/0029-5515/28/12/001
5. Heidbrink W. W., Chrien R. E., and Strachan J. D. 1983 Nucl. Fusion **23** 917. https://doi.org/10.1088/0029-5515/23/7/005
6. Hoek M., Bosch H.-S., and Ullrich W. "Triton burnup measurements at ASDEX Upgrade by neutron foil activation," IPP-Report IPP-1/320, 1999. https://www.osti.gov/etdeweb/biblio/356639
7. Batistoni P. et al 1987 Nucl. Fusion **27** 1040. https://doi.org/10.1088/0029-5515/27/6/017
8. Duong H. H. and Heidbrink W. W. 1993 Nucl. Fusion **33** 211. https://doi.org/10.1088/0029-5515/33/2/I03
9. Nishitani T. et al 1996 Plasma Phys. Control. Fusion **38** 355. https://doi.org/10.1088/0741-3335/38/3/010
10. Jungmin J. et al 2016 Rev. Sci. Instrum. 87 11D828. https://doi.org/10.1063/1.4961273
11. Ogawa K. et al 2019 Plasma Sci. Technol. **21** 025102. https://doi.org/10.1088/2058-6272/aaeba8
12. Wurden G. A et al 1995 Rev. Sci. Instrum. **66** 901. https://doi.org/10.1063/1.1146200
13. Nishitani T. et al 1997 Fusion Eng. Des. **34-35** 563. https://doi.org/10.1016/S0920-3796(96)00621-7
14. Takeiri, Y. 2018 IEEE Trans. Plasma Sci. **46** 2348. https://doi.org/10.1109/TPS.2017.2784380
15. Takeiri Y. et al 2018 IEEE Trans. Plasma Sci. **46** 1141. https://doi.org/10.1109/TPS.2017.2771749
16. Osakabe M. et al 2018 Fusion Sci. Technol. **72** 199. https://doi.org/10.1080/15361055.2017.1335145

17. Isobe M. et al 2018 Nucl. Fusion **58** 082004. https://doi.org/10.1088/1741-4326/aabcf4
18. Ogawa K. et al 2018 Plasma Phys. Control. Fusion **60** 044005. https://doi.org/10.1088/1361-6587/aaab1f
19. Ogawa K. et al 2018 Nucl. Fusion **58** 044001. https://doi.org/10.1088/1741-4326/aaab18
20. Ogawa K. et al 2020 Nucl. Fusion **60** 112011. https://doi.org/10.1088/1741-4326/ab6da0
21. K. Ogawa et al (2018) Plasma Fusion Res. **13**, 3402068. https://doi.org/10.1585/pfr.13.3402068
22. S. Sugiyama et al., Nucl. Fusion **60**, 076017 (2020) https://doi.org/10.1088/1741-4326/ab90c9
23. Nuga H. et al 2020 J. Plasma Phys. **86** 815860306. https://doi.org/10.1017/S0022377820000525
24. Ogawa K. et al 2018 Nucl. Fusion **58** 034002. https://doi.org/10.1088/1741-4326/aaa585
25. Takada E. et al 2016 Plasma Fusion Res. **11** 2405020. https://doi.org/10.1585/pfr.11.2405020
26. Isobe M. et al 2018 IEEE Trans. Plasma Sci. **46** 2050. https://doi.org/10.1109/TPS.2018.2836987
27. Ogawa K. et al 2018 Plasma Phys. Control. Fusion **60** 095010. https://doi.org/10.1088/1361-6587/aad4b7
28. Ogawa K et al 2021 Plasma Fusion Res. **16** 1102023. https://doi.org/10.1585/pfr.16.1102023
29. Du X. D. et al 2015 Nucl. Fusion **56** 016002. https://doi.org/10.1088/0029-5515/56/1/016002
30. Bando T. et al 2018 Nucl. Fusion **58** 082025. https://doi.org/10.1088/1741-4326/aac699
31. Ogawa K. et al 2018 Rev. Sci. Instrum. **89** 113509. https://doi.org/10.1063/1.5054818
32. Ogawa K. et al 2018 Rev. Sci. Instrum. 89 11I101. https://doi.org/10.1063/1.5032118
33. Koschinsky J. P. et al 2020 Contrib. Plasma Phys. **60** e201900186. https://doi.org/10.1002/ctpp.201900186
34. Ogawa K. et al 2020 Plasma and Fusion Research **15** 2402022. https://doi.org/10.1585/pfr.15.2402022
35. Ogawa K. et al 2021 Plasma Physics and Controlled Fusion **63** 045013. https://doi.org/10.1088/1361-6587/abe054
36. Takada E. et al 2019 Rev. Sci. Instrum. **90** 043503. https://doi.org/10.1063/1.5074131
37. Murata I. 2014 IAEA-TECDOC-1743 Compendium of Neutron Beam Facilities for High Precision Nuclear Data Measurements (Vienna: IAEA) pp 110–18 (https://www-nds.iaea.org/publications/tecdocs/iaea-tecdoc-1743/)
38. Isobe M. et al 2014 Rev. Sci. Instrum. 85 11E114. https://doi.org/10.1063/1.4891049
39. D. Ito et al., Plasma and Fusion Research **16**, 1405018. (2021). https://doi.org/10.1585/pfr.16.1405018
40. Nishitani T. et al 2017 Fusion Eng. Des. 136 Part A 210. https://doi.org/10.1016/j.fusengdes.2018.01.053
41. Ogawa K. et al 2019 Nucl. Fusion **59** 076017. https://doi.org/10.1088/1741-4326/ab14bc

Publisher's Note